Climate Dynamics (1991) 5:135-143

Climate Dynamics

A comparative study of the observations of high clouds and simulations by an atmospheric general circulation model*

RT Wetherald, V Ramaswamy, and S Manabe

Geophysical Fluid Dynamics Laboratory/NOAA, Princeton University, P. O. Box 308, Princeton, NJ 08542, USA

Received January 15, 1990/Accepted October 18, 1990

Abstract. The importance of clouds in the upper troposphere (cirrus) for the sensitivity of the Earth's climate e.g., requires that these clouds be modeled accurately in general circulation model (GCM) studies of the atmosphere. Bearing in mind the lack of unambiguous quantitative information on the geographical distribution and properties of high clouds, the simulated distribution of upper tropospheric clouds in a spectral GCM is compared with several satellite-derived datasets that pertain to high clouds only, for both winter and summer seasons. In the model, clouds are assumed to occupy an entire gridbox whenever the relative humidity exceeds 99%: otherwise the grid box is assumed to be free of cloud. Despite the simplicity of the cloud prediction scheme, the geographical distribution of the maxima in the model's upper tropospheric cloud cover coincides approximately with the regions of the observed maxima in the high cloud amount and their frequency of occurrence (e.g., intertropical convergence zone and the monsoon areas). These areas exhibit a minimum in the outgoing longwave radiation (OLR; Nimbus-7) and are also coincident with regions of heavy precipitation. The model, with its relatively simple cloud formation scheme, appears to capture the principal large-scale features of the tropical convective processes that are evident in the satellite and precipitation datasets, wherein the intense, upward motion is accompanied by condensation and the spreading of thick upper tropospheric layers of high relative humidity and cloudiness in the vicinity of the tropical rainbelt regions.

Introduction

The results from several numerical experiments conducted at various institutions have indicated that the feedback process involving cloud cover may enhance the sensitivity of climate to a forcing such as an increase of atmospheric carbon dioxide (e.g., Schlesinger and Mitchell 1987). For example, a recent study of Wetherald and Manabe (1988) demonstrated that the reduction of outgoing terrestrial radiation due to the increased altitude of high cloud plays an important part in enhancing the CO_2-induced warming of climate. It is therefore desirable to ascertain the extent to which a general circulation model (GCM) of climate is capable of simulating the present-day observed climatological characteristics of high clouds. These characteristics include the seasonal and geographical distribution of their locations and their areal coverage.

Unfortunately, it has proved very difficult to obtain unambiguous, quantitative information on the distribution of clouds in the upper troposphere. This may explain why very few assessments of high clouds, as simulated by GCMs, are available despite the potential importance of such clouds in controlling the sensitivity of climate. Notwithstanding this limitation, this study attempts to evaluate the simulated high clouds in the light of several satellite-derived datasets that have focussed on high clouds. These include studies by (a) Woodbury and McCormick (1986) on the frequency distributions of high cloud, as observed by the stratospheric aerosol and gas experiment (SAGE) satellite instrument, (b) Stowe et al. (1989) regarding cloud amounts as obtained from the NIMBUS-7 global cloud climatology experiment, (c) Kyle et al. (1986) on the outgoing longwave radiation (OLR) obtained from the NIMBUS-7 Experiment, (d) Barton (1983) on the frequency of high-level clouds using the selective chopper radiometer (SCR) aboard NIMBUS-5 and (e) Prabhakara et al. (1988) on the presence of thin cirrus clouds as obtained from the IRIS instrument aboard NIMBUS-4. With the exception of (a), all other studies have made use of nadir sounding devices. The SAGE system, in contrast, employed a limb-scanning technique that permitted detection of only those clouds that are present in the upper troposphere. (a), (b), (d) and (e) enable the assessment of cloud areal distributions while (c)

* This paper was presented at the International Conference on Modelling of Global Climate Change and Variability, held in Hamburg 11-15 September 1989 under the auspices of the Meteorological Institute of the University of Hamburg and the Max Planck Institute for Meteorology. Guest Editor for these papers is Dr. L. Dümenil

enables an assessment of cloud heights and longwave radiative properties. Since the existence of high cloud results in the marked reduction of OLR from the top of the atmosphere, a good simulation of the characteristics of high cloud is necessary for the successful reproduction of the outgoing radiation. Barton and Prabhakara et al. [(d) and (e) respectively] developed algorithms, based upon radiative effects of high clouds, to extract the frequency of occurrence from satellite radiance measurements. In particular, (d) concentrated on extracting thin cirrus clouds that were well removed from the dense storm centers; studies (d) and (e) complement the study in (a).

The large-scale, cloud-related features appearing in the observed satellite and precipitation datasets are analyzed, with an emphasis on the high clouds occurring as part of the tropical convective systems. As noted, an important limitation arising for the "high" clouds, particularly for thin optical depths, is the difficulty in obtaining an unambiguous inference of their distribution and physical properties. Although this factor renders comparative studies necessarily qualitative in nature, we adpot the approach of considering several different datasets on high clouds, with a view toward ascertaining the large-scale features of these clouds, and investigating the consistency between the various datasets in forming a coherent picture of the areal distributions of these clouds during the different seasons. The chief objective of the present investigation is to compare the simulated climatological, large-scale features of high clouds from a GCM having an interactive cloud prediction scheme with the results emerging from the above-mentioned datasets. Unlike earlier GCM studies (e.g., Ramanathan et al. 1983) that consider the simulations of clouds in general, the focus of this study is solely on high clouds.

Simulation experiment

Model structure

The model is a semi-spectral model and is, essentially, the same as that described in Manabe et al. (1979) and Manabe and Hahn (1981) except that it incorporates a simplified method of cloud prediction. The model is rhomboidally truncated at wave number 15 and has 9 vertical finite difference levels.

Precipitation is computed whenever supersaturation is indicated by the prognostic equation for water vapor. The moist convective processes are parameterized by a moist convective adjustment scheme proposed by Manabe et al. (1965). Based upon observation, the seasonal and geographical distributions of sea surface temperature and sea ice coverage are prescribed. The temperature of the continental surface is computed from the condition of local thermal equilibrium among the various components of surface heat balance. Surface hydrology is determined by the "bucket" method described in Manabe (1969). The soil albedo is prescribed geographically but is replaced by a higher value over snow-covered regions.

Insolation is prescribed over the annual cycle. The method for computing it is similar to that proposed by Lacis and Hansen (1974). Terrestrial radiation is computed by the method described by Rodgers and Walshaw (1966) and modified by Stone and Manabe (1968). In addition, the effect of the water vapor continuum has been incorporated into the radiation code. For the computation of both solar and terrestrial radiation, the standard value of the atmospheric CO_2-concentration was assumed and a zonally uniform O_3-distribution was prescribed as a function of latitude, height and season. Random overlapping is assumed for all clouds in the radiative computation.

The prognostic scheme of cloud cover is basically the same as that used in the previous studies of Wetherald and Manabe (1980, 1988). In these studies, it is assumed that all condensed water precipitates out of the layer and is not retained as cloud liquid water. Nevertheless, overcast cloud is predicted when the relative humidity of air exceeds a critical value. This relative humidity criterion is applied to all clouds, both convective and non-convective, regardless of where they occur in the global domain. The value of this critical relative humidity was chosen to be 99% based upon the amount of total cloud, not just high cloud alone. The above choice of critical relative humidity resulted in a total global cloud amount of approximately 50%. The absorption and reflection of solar radiation by various cloud types are described in Wetherald and Manabe (1988) and are listed in Table 1 of their paper. For the computation of terrestrial radiation, all clouds, including high (e.g., cirrus) clouds, are considered to be completely black bodies.

Time integration

Starting from an initial condition of an isothermal dry atmosphere at rest, the model was integrated with a prescribed sea surface temperature distribution for the standard value of the solar constant until a quasi-equilibrium climate was reached. The model was then integrated for an additional 10 model years to provide a suitable analysis period. The computed cloud distributions illustrated in this paper are generated from averages taken over this 10 year analysis period.

Analysis of the results

Zonal mean cloudiness

It is useful to examine first the distribution of zonal mean cloud amount which is obtained from the model. This is shown in Fig. 1 and indicates that a thick layer of relatively greater cloudiness occurs in the upper troposphere of the model. The altitude of this high cloud layer decreases with increasing latitude in a manner analogous to the height of the tropopause. The thick layer of cloudiness in the upper model troposphere may be identified as "cirrus" cloud and corresponds

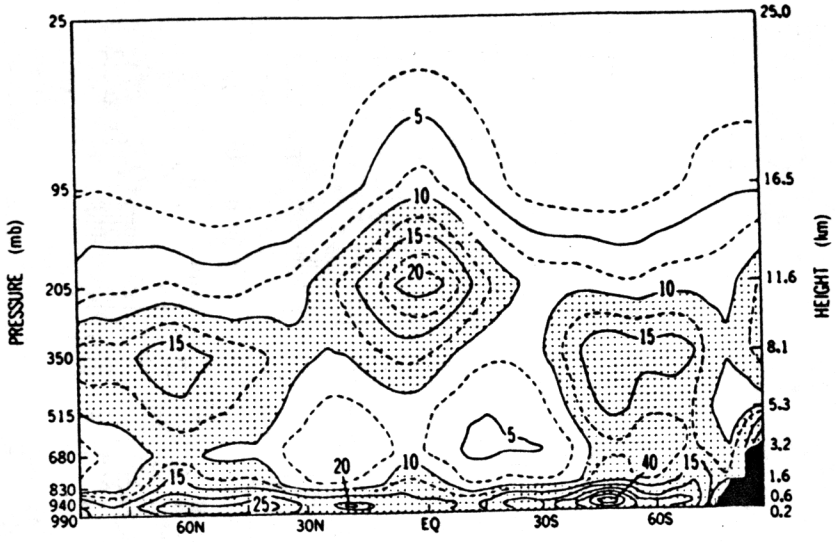

Fig. 1. Latitude-height distribution of the annual zonal mean cloud amount (%) obtained from the GCM

well to the latitudinal variation of the height of cirrus cloud as determined by London (1957) (see Fig. 12 of Wetherald and Manabe 1980). An exception to this is in the tropics where the model produces cirrus clouds which are at a considerably greater altitude than the ones determined by London.

One may also note that the regions of maximum high cloud amount correspond closely to the annual mean positions of both the tropical and middle latitude rainbelts. It is in these regions where moist, saturated air is carried upwards until it reaches the upper troposphere where it has a tendency to spread horizontally.

High cloud amount

The computed high clouds in the atmosphere are assumed to occur at levels 2, 3 and 4 of the 9 level model, namely at 95, 205 and 350 mb located at the altitudes of 16.5, 11.6 and 8.1 km, respectively. Since level 5 in the model is considerably lower (5.3 km) than the altitude limit of high clouds considered by Stowe et al. (7 km), only levels 2-4 are considered for comparison with observations.

The geographical distributions of high cloud amount as obtained from (a) the simulation and (b) Stowe et al.'s observations are shown in Fig. 2 for December-February conditions. Generally speaking, the model overestimates the amount of high cloud in low latitudes, particularly over Africa, the Indonesian region and over South America. Note that the shading begins from a lower contour value for the observations. The tongue of cloudiness extending from the equatorial belt to a band east of Australia (the southern Pacific convergence zone) appears more pronounced in the observations than in the model. This appearance is due to high clouds filling the entire equatorial zone in the model; in particular, there is considerably more cloudiness in the model along the equator, between longitude 150° W and 90° W, while the observations indicate a near absence.

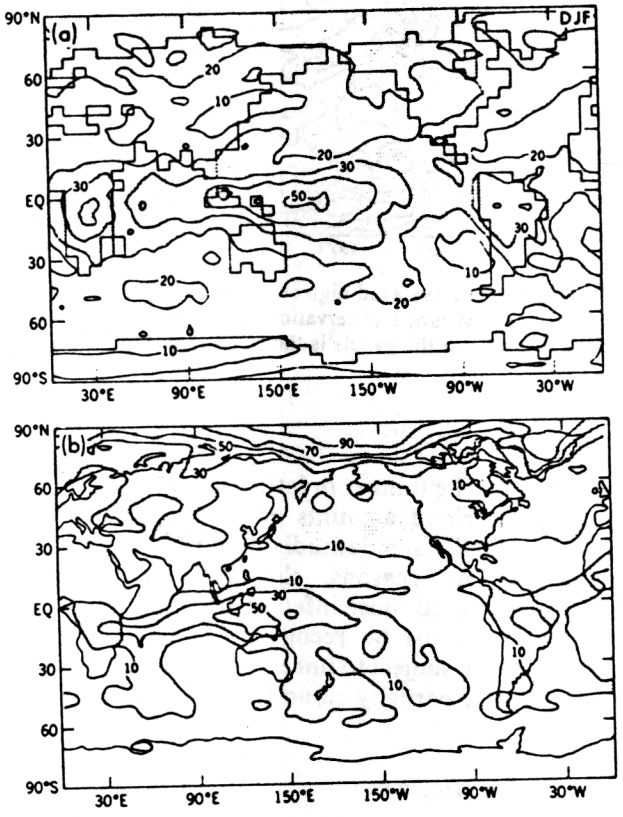

Fig. 2a, b. Time-averaged high cloud amount (%) for December-February: a a 10-year GCM run; b observations by Stowe et al. (1989) for January 1980. Note the difference in shading between a and b

For the June-August simulation (Fig. 3a, b) the main convective zone over Asia and in the Caribbean are represented successfully by the model. The northward extension of the intertropical convergence zone (ITCZ) is prominent in both the observations and the model results. Again, the simulated cloud amounts exceed those of the observed distributions over the convective zones. The equatorial belt of high cloudiness is

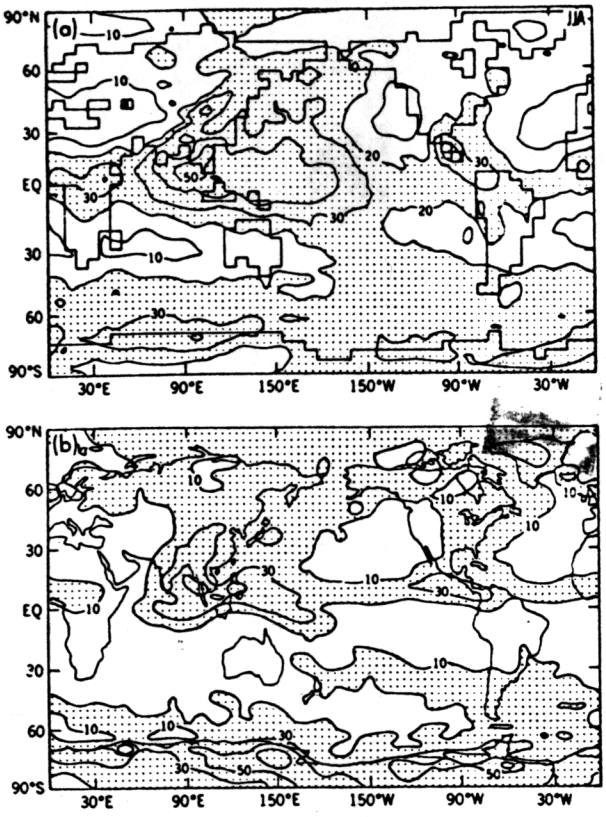

Fig. 3a, b. Time-averaged high cloud amount (%) June-August: **a** a 10-year GCM run; **b** observations by Stowe et al. (1989) for July 1979. Shading in the panels is the same as in Fig. 2

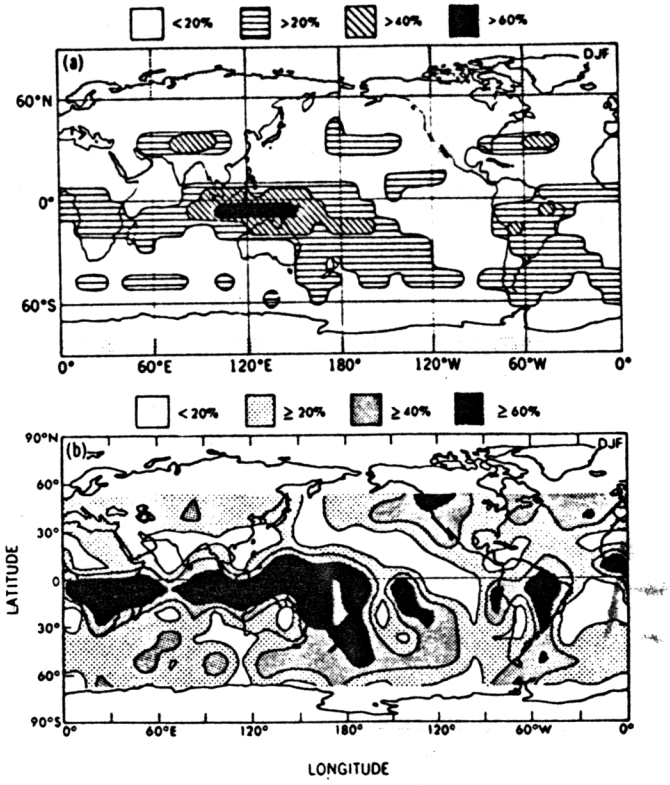

Fig. 4a, b. Geographical distribution for the period of December-February of the: **a** frequency of high cloud occurrences (%) as obtained by Woodbury and McCormick (1986) (measurements taken over the years of 1979 to 1981); **b** those obtained by Barton (1983). Legends for the different percentage categories are designated as various shades at the top of each figure

observed to be thinner in latitudinal extent; in contrast, the GCM cloud amounts occupy a larger area, both longitudinally and latitudinally. For both the winter and summer seasons, the computed high cloud amounts exceed those inferred from the satellite observations. It must be recognized that observed cloud amounts are subject to uncertainties related to the interpretation of partially cloud-filled pixels.

High cloud frequency

Next, the frequency of high cloud simulated by the model is compared with the frequency of its appearance obtained from the SAGE and NIMBUS-5 measurements. In the analysis of the SAGE extinction measurements, Woodbury and McCormick (1986) assumed that high clouds appear in an altitude zone bounded by the tropopause plus 1 km as an upper limit and 70% of the tropopause height or 8 km (whichever is greater) as a lower limit. The definition of the tropopause altitude was identical to that used by the National Meteorological Center and corresponds approximately to the high cloud's height definition used by Stowe et al.

While the frequency of occurrence of cirrus clouds and the time-averaged cloud amount cannot be compared in a quantitative sense, it is nevertheless instructive to examine the correlation between the patterns appearing in the respective datasets. The SAGE-derived geographical distribution of the high cloud frequency averaged over the three-month period of December, January and February is shown in Fig. 4b. In low latitudes, the shaded areas of Fig. 2, which include regions of high cloud amount maxima in the model atmosphere and observation, compare quite well with the dark areas of Fig. 4 where the appearance of high cloud is observed to be most frequent. For example, the most intense cloudy area over the Amazon River basin and the dark equatorial belt associated with the ITCZ extends all the way from Africa to the central Pacific Ocean in both Figs. 2 and 4b, although, as noted previously for cloud amount, the observed belt is not as continuous over the Indian Ocean as it is for the computed distribution. Figure 4a shows Barton's inferred high cloud frequencies. There is a good overlap of the cirrus cloud locations in Barton's data with that of Woodbury and McCormick. The maxima in the first dataset does, indeed, coincide with the maxima in the latter. Both the datasets show the tongue of cloudiness enveloping the ITCZ, although the SAGE pattern indicates a higher frequency. As indicated by the observed cloud amount in Figs. 2b and 3b, Barton's dataset shows the absence of high clouds in the 150° W-90° W longitude region of the equatorial belt; in contrast, SAGE suggests that

some portions of this region do, however, have at least a 20% frequency of occurence.

A good correspondence is also noted between Figs. 3 and 5 which make a similar comparison for the three-month period of June, July and August. In both Figs. 5b and 3, the dark and shaded areas over the Indian Ocean and the western Pacific Ocean extend northwards from the vicinity of the ITCZ in the equatorial region to middle latitudes.

Figure 5a shows Barton's high cloud frequency of occurrences for the June–August season. The correspondence with the SAGE system is good although, once again, it exhibits magnitudes that are considerably (up to a factor of two) less than those obtained by the limb-detection technique.

In general, there is a considerable underestimate in the Barton dataset relative to SAGE. This occurs despite the fact that the Barton dataset has a lower cutoff altitude (6 km) for the classification of high clouds. As noted by Woodbury and McCormick (1986), this could be due to the fact that the SAGE consists of a limb scanning device and, therefore, the instrument is saturated for even small extinctions. Because of this, it is likely to detect even the thinnest of clouds. The SCR, on the other hand, since it is a nadir scanning instrument, lacks the sensitivity of the SAGE limb scanning device. However, the co-locations of the maxima exhibited in the independent datasets are extremely encouraging since they indicate the unambiguous presence of the high clouds. Thin cirrus clouds could explain the relatively low frequency values in the Barton dataset, particularly for cirrus cloud occurrences corresponding to the 40% values of the SAGE dataset. Note that while SAGE can detect upper tropospheric clouds directly, the screening in Barton's technique involves empirical analyses. Another interesting point is that the geographical positions of the SAGE maxima are unlikely to be altered due to changes in the detection threshold.

The SAGE and Barton datasets deteriorate in quality poleward of 50° latitude in both hemispheres due to the relatively shallow slant angle of the scanning sensor and a lowering of the tropopause and the cloudtop altitude in high latitudes. It should also be borne in mind that the different sampling times and the unequal number of samples in the two datasets could also be partly responsible for the differences in the frequencies of occurrence.

It is pointed out at this stage that, the location of some cirrus clouds well removed from the core of the tropical convective systems, as inferred by Prabhakara et al. using radiances in two spectral channels (not shown here), corroborates the observation of Barton, Woodbury and McCormick, particularly in those regions which have minimum-to-moderate frequency values (approximately 20 to 40%) in the latter two datasets. Stowe et al. have indicated comparatively good agreement of their observations with the Barton dataset, with only a few exceptions indicating an underestimate.

From Figs. 2–5, there is good agreement between the observed and computed distributions of high cloud cover in the low and middle latitudes during the summer months, particularly in the Northern Hemisphere summer season. However, there are two notable exceptions to this; over the ocean east of Australia during December, January and February and over the United States during June, July and August. In both cases, the regions of maximum observed high cloud frequency and high cloud amount exhibit a tongue-like feature extending poleward from the equatorial convective regions, which is not as pronounced in the GCM simulated patterns. These two examples will be dealt with in more detail in the succeeding subsections.

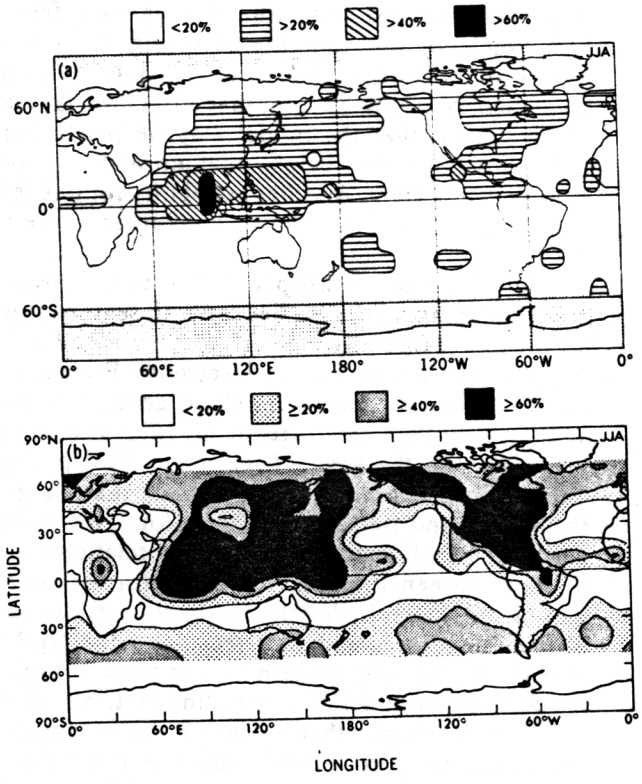

Fig. 5a, b. Same as Fig. 4 except for the period of June–August

Outgoing longwave radiation (OLR)

The cloud amount and frequency data discussed above indicate intrinsic characteristics of high cloud distributions but do not enable an evaluation of the cloud radiative characteristics. One approach to estimate these lies in using the OLR data. Here, a comparison is made between the simulated and observed distributions of the OLR at the top of the atmosphere. Since the effective temperature for the upward emission from high cloud is very low, the existence of high cloud tends to imply a smaller OLR as compared with regions of either clear sky or lower cloud types. Thus, realistic simulations of both the amount and optical properties of high cloud cover are necessary for an accurate reproduction of the OLR by a model. Fig. 6 compares the geographical distribution of the OLR from the model with the corresponding distribution of the actual OLR

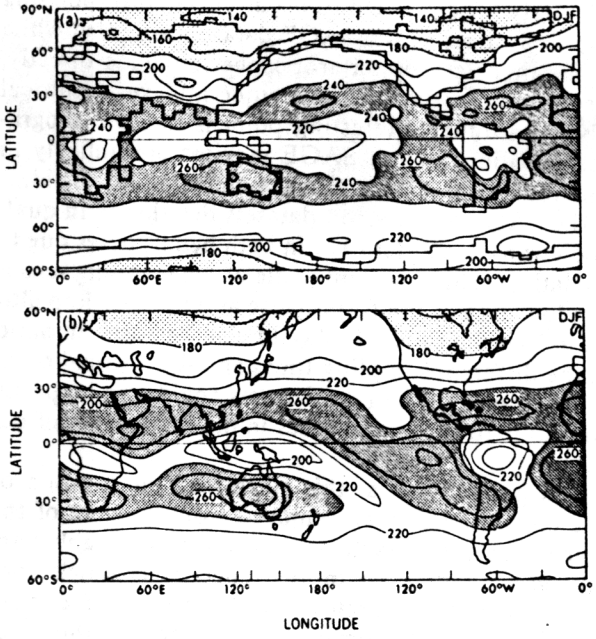

Fig. 6a, b. Geographical distribution for the period of December-February of the net outgoing terrestrial radiation at the top of the atmosphere (W/m^2) obtained from: **a** the GCM; **b** the NIMBUS-7 ERBE satellite system for 1981. Source is Kyle et al. (1986)

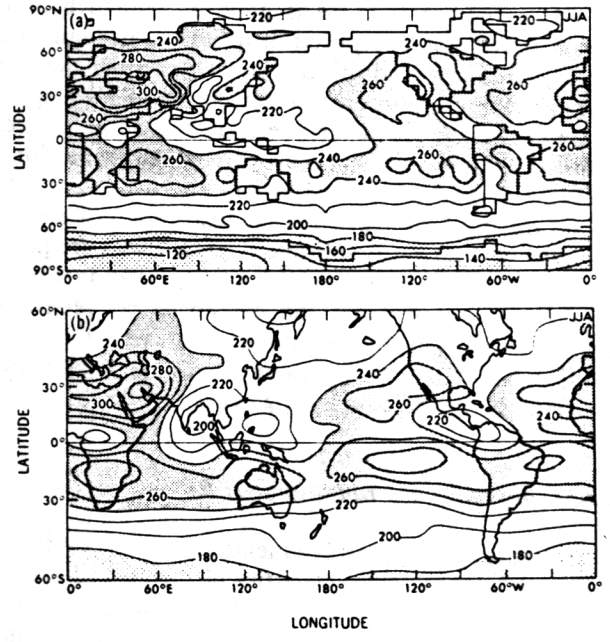

Fig. 7a, b. Same as Fig. 6 except for the period of June-August

as determined from the NIMBUS-7 satellite observations (Kyle et al. 1986) for the period of December, January and February 1981. In Fig 6, the patterns of shaded (maxima) and unshaded (minima) regions compare quite well between the model and the observations. For example, the regions of minimum emission (< 200 W/m^2) in the vicinity of the equator over Africa, South America and the western Pacific Ocean are apparent in both figures. Also apparent in both figures are the regions of maximum emission north and south of the equator, particularly over Australia, the south Atlantic and Pacific Oceans, and off the western coasts of Africa and South America. There is, however, more zonality evident in the computed distribution as compared with the observations.

Turning to Fig. 7 which illustrates the same quantities for the period of June, July and August, one may again note the close correspondence between the computed and observed distributions of OLR. An example of this is the region of low OLR beginning at the equator, particularly over the Indian and western Pacific Oceans, and extending northward into middle latitudes. Much smaller regions of minimum emission exist over equatorial Africa and Central America in both Figs. 6 and 7. The areas of maximum OLR off the western coasts of North America and South America as well as Europe and western Asia are in good qualitative agreement with each other. Taken together, these results indicate that the geographical pattern of the OLR at the top of the atmosphere in the tropics is reasonably well simulated by the model.

In general, the GCM results exhibit more zonality in low latitudes as compared with the SAGE and NIMBUS-7 data. This is more prominent in the December-February months. These features can be seen, for example, in the comparison of the cloud amont and occurrence maxima (Figs. 2, 4) and the OLR minima (Fig. 6) over the western Pacific. Furthermore, the band of high cloudiness extending from the western Pacific into the middle latitudes of the Southern Hemisphere is less pronounced in the model. There is a systematic overestimation of OLR by the GCM in the unshaded (cloudy) regions of the tropics as compared with the NIMBUS-7 results. This suggest that, either there are too few thick high clouds, or that they are occurring at too low an altitude in the model. Also, there is a systematic underestimation of OLR in the shaded (clear sky) areas which suggest that the model may be producing too many clouds in the regions that normally would be clear or nearly clear. Another possibility for this feature is an underestimate of relative humidities in the model.

The direct relationship between cloud cover and OLK evident in all the studies for both seasons is worth highlighting especially in the latitude zone of 30° S to 30° N. In particular, for the December-February period, the regions of maximum cloud amount in Fig. 2b and the maximum cloud frequency (Fig. 4) correspond very closely to the areas of minimum OLR in Fig. 6b. This is consistent with the expectation that the greater the amount and frequency of high cloud, the lower the amount of OLR emission. A similar relationship may be seen between Figs. 3b, 5b and 7b for the June-August period. Here, both datasets show an extensive area of high cloudiness and its effect upon the OLR field over the Indian and western Pacific Oceans beginning in equatorial latitudes and extending up to about 50° N. These results suggest that not only is the maximum high cloud frequency co-located with the maximum high cloud amount in the tropics but that both are anti-cor-

related with the corresponding OLR observations for the same time period. Thus, the latter dataset may be useful in identifying the occurences of high cloud cover over time and space, especially in low latitudes.

In the GCM results, a similar relationship exists between the computed high cloud amount and the accompanying OLR at the top of the model atmosphere. Again, there is a close correspondence between the shaded areas of Figs. 2a (maximum high cloudiness) and the unshaded regions of Fig. 6a (minimum emission), as well as between the shaded areas of Fig. 3a and the unshaded regions of Fig. 7a. Thus, the GCM simulation of high cloud cover and terrestrial radiation not only corresponds well with the respective observed data but also reproduces the correlationship between these two quantities as indicated by the independent sets of observations.

It is of interest to examine both the computed and observed OLR in the region east of Australia during December, January and February, and over the United States during June, July and August where the maximum in cloud frequency and amount exhibit more of a poleward extension than the computed cloud amount. An examination of these two regions reveals that the area of observed minimum OLR which extends southeastward from equatorial latitudes east of Australia is not reproduced by the model. On the other hand, in both the observations and the model there is no indication of a minimum in OLR over the United States. This suggests that the region of maximum observed amount and frequency of high clouds, which also extend southeastward from tropical latitudes to east of Australia, consists of thick clouds that reduce the OLR, whereas the cloud cover over the United States possibly consists mainly of thinner high clouds that do not greatly affect the OLR there.

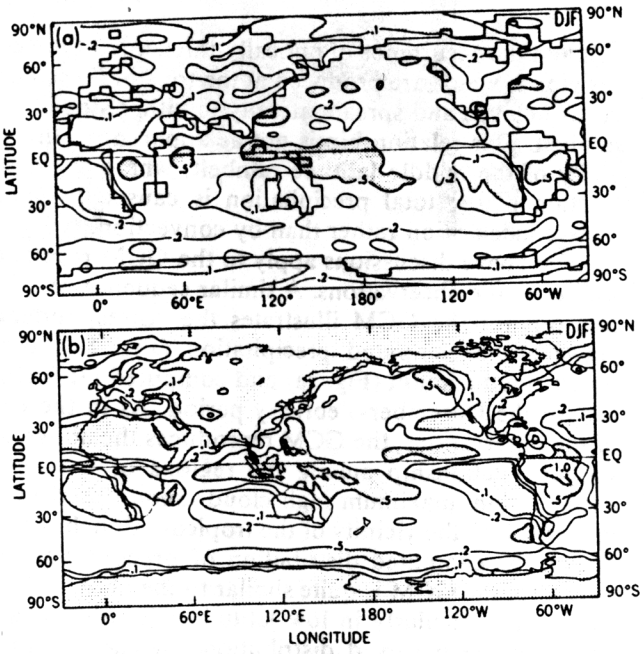

Fig. 8a, b. Geographical distribution of total precipitation (cm/day) for the period of December-February obtained from: a the GCM; b Jaeger (1976)

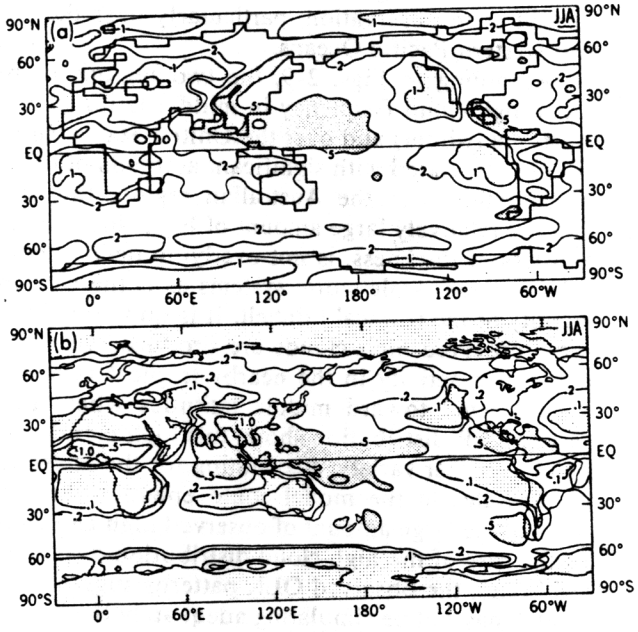

Fig. 9a, b. Same as Fig. 8 except for the period of June-August

Precipitation

For either the computed or observed case, the regions of minimum OLR include the tropical rainbelt which implies that these areas contain mostly optically-thick high clouds associated with deep convective processes rather than the more optically-thin cirrus clouds not necessarily associated with convection. Consider the observations first. Figs. 8 and 9 show the observed distribution of total precipitation rate (Jaeger 1976) for both the December-February period (Fig. 8) and the June-August period (Fig. 9b). The maxima in the two observed high cloud distributions (Figs. 2b, 4b and 6b, respectively) correspond very closely with the regions of maximum precipitation amount associated with the tropical rainbelt for both seasons. Specifically, the tropical rainbelt shown in Fig. 8b coincides with the dark regions of maximum cloud amount in Fig. 2b over the Pacific and Indian Oceans as well as over South America. A similar relationship may be seen for Figs. 9b and 3b where the tropical rainbelt over the Indian and western Pacific Oceans and over Central America coincide with the dark areas of maximum high cloudiness in these regions. An examination of these figures reveals that, in the western Pacific, the northward extension of the region of tropical rainfall is accompanied by a corresponding northward extension of the area of maximum high cloudiness associated with the region of tropical rainfall. In fact, Newell et al. (1974) have shown that the tropical distributions of cloudiness and rainfall maxima are well correlated with the maxima in the 500 mb vertical velocity fields. These facts, taken together, indicate that a direct relationship exists between the intense upward motions in the tropical rain-

belt and the occurrence of optically-thick anvil-type cirrus clouds which are produced at the tops of these convective clouds and spread laterally to either side of the rainbelt. This relationship is not as apparent in the vicinity of the middle latitude rainbelt, where a greater fraction of the total precipitation is caused by large scale condensation rather than by convection.

The above discussions apply to the GCM results as well as to the observations. A similar sequence of comparisons for the GCM illustrates the correspondence between the computed precipitation (Fig. 8a), computed cloud amount (Fig. 2a) and computed OLR (Fig. 6a) for the December-February period. As in the case of the observations, the GCM reproduces the above described relationship among the regions of maximum precipitation, maximum high cloud amount and minimum OLR in the vicinity of the tropical rainbelt. In addition, the computed distribution of precipitation obtained for the GCM is quite similar to the observed distribution particularly in low latitudes. Besides, it also simulates the observed distributions of each of these quantities quite well. Similar remarks apply to the computed June-August distributions of precipitation, cloudiness and terrestrial emission (Figs. 3a, 7a and 9a, respectively) with regard to consistency within the model as well as to observation, particularly over the Indian and western Pacific Oceans.

According to Figs. 2-9, the two regions of maximum high cloud frequency in middle latitudes east of Australia (winter) and over the United States (summer) are not associated with significant amounts of observed precipitation. For the Australian region, this implies that the relatively large amount of high cloud cover, regardless of thickness, is not overlying deep convective cells or larger scale storm systems as is the case in the vicinity of the tropical rainbelt. It is quite possible that these observed high clouds are produced by the deep convective activity in the nearby tropical rainbelt and are advected toward middle latitudes where the observed OLR distribution shows this high cloud cover to be of a thicker variety. Accounting for the advection of condensates in the model could enhance the simulations of the large amount of observed high clouds there. In the case of the high cloud distribution over the United States, the observed OLR patterns suggest that the model may not be simulating adequately the horizontal extent of the high clouds.

Conclusions and discussion

The present study demonstrates that satellite data on the amounts and frequency of occurrences of cirrus clouds, together with that of the outgoing terrestrial radiation, are useful for an assessment of the simulation of high clouds by a GCM. Despite the fact that the various satellite datasets have employed different techniques to infer the distribution of high clouds, all the datasets are in agreement with respect to the location of upper tropospheric clouds in the tropics. In particular, the highest amounts and frequencies of occurrence of cirrus clouds, as revealed by the independent datasets, are co-located over the intensely active convective regions. The frequency of occurrence of high clouds estimated by the solar occultation technique exceeds that obtained by the nadir scanning technique. This could be due to differences in the altitude limits used to classify high clouds, or sampling problems. A more likely cause may be the differences in the detection technique. The higher sensitivity normally associated with the limb scanning technique (Woodbury and McCormick 1986) suggests that it would be sensitive to even extremely thin cirrus clouds.

Since both the limb and the nadir datasets yield high cloud frequencies over the convective regions as well as locations far removed from them, it becomes important to address their relevance for climate studies. This is so because such clouds can play an important role in affecting the longwave convergence within the atmosphere (Ramanathan 1987), in the general circulation (Ramaswamy and Ramanathan 1989) and in the modeled climate change (Wetherald and Manabe 1988) due to increases in trace gas concentrations. Are most of the clouds detected by the SAGE technique optically significant to cause an appreciable radiative effect or are they too thin to do so? If the former is the case, then their large areal coverage in the tropics all year around, as indicated by the SAGE observations, necessitates not only a continuous monitoring of their existence but also the development of accurate strategies for inferring their radiative properties.

At the present time, we lack a comprehensive picture of the quantitative aspects of "high" clouds, particularly their radiative properties. Nadir scanners, typically, cannot unambiguously infer the emissivity and distribution of high, thin clouds. Although the limb scanning technique is useful for separating out the high clouds from other middle and lower tropospheric clouds, the fact that these measurements, too, cannot yield an unambiguous determination of cirrus optical properties limits their potential at present.

The comparison of the frequency of occurrence and NIMBUS-7 datsets indicates a good correlation between maximum high cloud frequency and minimum OLR at the top of the atmosphere, which can be exploited in future observational studies. The absence of quantitative information on "high" clouds is a severe impediment in assessing the simulations from a GCM comprehensively. Nonetheless, by comparing several different sources of data on high clouds and precipitation in this study, it has been possible to evaluate the qualitative adequacy of the simulations. Despite the extreme simplicity of the cloud prediction scheme employed in the GCM (same value of critical relative humidity for cloud formation is used at all altitudes and latitudes), the model appears to simulate not only the qualitative features of the global distributions of high clouds, but also their influence upon the OLR at the top of the atmosphere. For both the GCM and observed data, the geographical patterns of cloud cover maxima, OLR minima and precipitation maxima in the tropics are all highly correlated. Although the model

exhibits an underestimate of the OLR minima, it appears to capture the essence of the large-scale features of tropical moist convection evident in the observations. This is particularly true where intense upward motions are accompanied by condensation and the spreading of a thick upper tropospheric layer of high relative humidity and large cloudiness in the vicinity of the tropical rainbelt region. To this extent, the simplicity of the cloud prediction scheme and its qualitative success suggests that the basic physical processes involved in the large-scale distribution of the tropical high clouds may be adequately represented in the present GCM simulations. This constitutes the principal finding of this study.

From the comparative studies performed here, the model simulations exhibit an underprediction of the cloudtop altitude, especially in the vicinity of the tropical convective regions. Remedies for these may involve sub-grid scale parameterizations of moist convection (e.g., from the FIRE experiments), higher vertical and horizontal resolution (ongoing projects at several institutions) and prognostic equations for the condensed phase besides the one for water vapor. Also, in the future, attention needs to be paid to the emissivities of cirrus clouds, particularly in middle latitudes. In the tropics, the upper tropospheric clouds simulated by the present GCM may be representative of deep systems (either part of "hot" convective towers or anvil shields spreading out of a parent tower) and, thus, an emissivity of unity (equivalently, an assumption of 'black' cloud as in this study) may be realistic. The same argument cannot be applied readily to the mid-latitudes. Nonetheless, the results of this study, besides demonstrating that the combination of the different satellite and the precipitation datasets are useful in evaluating the large-scale climatological features of the GCM-simulated high clouds, also provide an encouragement to conduct quantitative comparisons with the physical properties of such clouds as and when they become available.

References

Barton IJ (1983) Upper level cloud climatology from an orbiting satellite. J Atmos Sci 40:435-447

Jaeger L (1976) Monthly precipitation maps for the entire earth (in German). Ber Dtsch Wetterdienstes 18:139

Kyle HL, Arduany PE, Hucek RR, The Nimbus-7 ERB Experiment Team (1986) El Niño and outgoing longwave radiation: An Atlas of Nimbus-7 Earth Radiation Budget Observations. NASA Reference Publication 1163

Lacis A, Hansen J (1974) A parameterization for the absorption of solar radiation in the earth's atmosphere. J Atmos Sci 31:118-133

London J (1957) A study of the atmospheric heat balance. Final Report, AFCRC Contract AF 19(122)-165, New York University (DDC AD 117227)

Manabe S (1969) Climate and the ocean circulation: I. The atmospheric circulation and the hydrology of the earth's surface. Mon Wea Rev 97:739-774

Manabe S, Hahn DG (1981) Simulation of atmospheric variability. Mon Wea Rev 109:2260-2286

Manabe S, Hahn DG, Holloway JL Jr (1979) Climate simulations with GFDL spectral models of the atmosphere: effect of spectral truncation. Rep of the JOC Study Conf on Climate Models: performance intercomparison and sensitivity studies, Washington DC, 3-7 April 1978. GARP Publ Ser No 22, Vol 1, 41-94 (NTIS N8027917)

Manabe S, Smagorinsky J, Strickler RJ (1965) Simulated climatology of a general circulation model with a hydrological cycle. Mon Wea Rev 93:769-798

Newell RE, Kidson JW, Vincent DG, Boer GJ (1974) The general circulation of the tropical atmosphere. Vol 2, Chap 9, MIT Press, Cambridge MA, USA

Prabhakara C, Fraser RS, Dalu G, Wu Man-li C, Curran RJ (1988) Thin cirrus clouds: Seasonal distribution over oceans deduced from Nimbus-4 IRIS. J Appl Meteor 27:379-399

Ramanathan V (1987) Atmospheric general circulation and its low frequency variance: Radiative influences. J Meteor Soc Japan 65:151-175

Ramanathan V, Pitcher EJ, Malone RC, Blackmon ML (1983) The response of a general circulation model to refinements in radiative processes. J Atmos Sci 40:605-630

Ramaswamy V, Ramanathan V (1989) Solar absorption by cirrus clouds and the maintenance of the tropical upper troposphere thermal structure. J Atmos Sci 46:2293-2310

Rodgers CD, Walshaw DC (1966) The computation of infra-red cooling rate in planetary atmospheres. Quart J R Meteorol Soc 92:67-92

Schlesinger ME, Mitchell JFB (1987) Model projections of the equilibrium climatic response to increased CO_2. Rev Geophys 25:760-798

Stone HM, Manabe S (1968) Comparison among various numerical models designed for computing infrared cooling. Mon Wea Rev 96:735-741

Stowe LL, Yeh HYM, Fox TF, Wellemeyer CG, Kyle HL, The NIMBUS-7 Cloud Data Processing Team (1989) Nimbus-7 global cloud climatology. Part II: First year results. J Climate 2:671-709

Wetherald RT, Manabe S (1980) Cloud cover and climate sensitivity. J Atmos Sci 37:1485-1510

Wetherald RT, Manabe S (1988) Cloud feedback processes in a general circulation model. J Atmos Sci 45:1397-1415

Woodbury GE, McCormick MP (1986) Zonal and geographical distributions of cirrus clouds determined from SAGE data. J Geophys Res 91:2275-2787